Some dense random packings generated by the dead leaves model

Dominique Jeulin

CENTRE DE MORPHOLOGIE MATHEMATIQUE
35, rue Saint-Honoré, 77305 FONTAINEBLEAU (FRANCE)

Some dense random packings generated by the dead leaves model

Dominique JEULIN

N-01/17/MM

Septembre 2017

Some dense random packings generated by the dead leaves model

Dominique JEULIN

28 September 2017

Abstract. The intact grains of the dead leaves model enables us to generate random media with non overlapping grains. Using the time non homogeneous sequential model with convex grains, theoretically very dense packings can be generated, up to a full covering of space. For these models are given the theroretical volume fraction, the size distribution of grains, and the pair correlation function of centers of grains.

1. Introduction

Packings of objects provide models for granular media. It is important for applications to get models showing a high volume fraction of grains. When using spheres with a single radius r, it is known that the highest volume fraction is 0.7404, corresponding to Kepler's conjuncture, which was proved by Th. Hales, as explained in [3]. In [4], up to 0.55 volume fraction of spheres with the same radius could be obtained, starting from a dense CFC (cubic face centered) ordered arrangement of spheres, and combining random deletion and translations of spheres. Simulations of systems of non-overlapping long fibers [1] were developped from a combination of random walks and of a combination of attractive and repulsing forces.

We will follow here a different approach, based on a probabilistic model of non overlapping objects obtained by means of the dead leaves model [11, 6], when considering grains which remain uncovered during the sequence [8]. When these grains are spherical with a single radius R, the centres of non-overlapping spheres produce a standard Hard-Core point process [10, 12]. Using the time homogeneous model provides random sets with a low volume fraction. Dense packings can be obtained when using convex grains with a size distribution, and appropriate sequences during the generation of the model. In what follows, the results obtained for the time homogeneous case are reminded, and some sequential versions are studied, for which dense packing (up to space filling) can be reached theoretically. Theoretical size distributions of grains generating these packings are provided. Finally the pair correlation functionof centers of grains is given

2. Intact grains of the dead leaves model for the time homogeneous case

We start from a sequence of random grains A' with volume $\mu_n(A')$ implanted in the n dimensional space according to a space-time point Poisson process with a constant intensity θ. During the sequence are kept only the grains falling outside of the earliest grains, namely the intact grains, which generate a random set $A(t)$. In a first step

is considered the case where a single symetric convex grain A' is used (for instance a sphere with radius R). The volume fraction (in $\mathbb{R}^3$) or more generally the probability $p(t)$ for a given point x to belong to the random set $A(t)$ is given by

$$p(t) = P\{x \in A(t)\} = \frac{1}{2^n}\left[1 - \exp(-\theta t 2^n \mu_n(A'))\right]. \tag{1a}$$

For $t \to \infty$, we get $p = \frac{1}{2^n}$. As a result, the intact grains of a dead leaves model generate a random set of non overlapping grains with a limited packing density (namely 0.5, 0.25, and 0.125 in $\mathbb{R}$, $\mathbb{R}^2$ and $\mathbb{R}^3$).

Proof. The event "$x \in A(t)$" can be written: at some $u < t$, x is covered by a random grain A' falling outside of the previous occurences of grains A' from time 0 to time u (generating a Boolean model with grain A' and with intensity θu). Therefore

$$p(t) = \int_0^t \theta \mu_n(A') \exp(-\theta u 2^n \mu_n(A')) du \tag{1b}$$

since $\mu_n(A' \oplus \check{A}') = 2^n \mu_n(A')$ for any symmetric convex set A'. ■

It turns out that replacing the single grain by a population of grains generates a random set with $p < \frac{1}{2^n}$, as conjectured in [2] and shown in [9], so that the time homogeneous model with a single grain provides an upper bound of the probability p.

3. INTACT GRAINS OF THE DEAD LEAVES MODEL FOR THE GENERAL CASE

3.1. Space fraction covered by the intact grains. We consider now a time sequence of random grains $A'(t)$ implanted on Poisson points with intensity $\theta(t)$. Keeping the grains of the sequence falling outside of previous grains gives a random set $A(t)$. The probability $p(t)$ is given below.

Theorem 1. *The probability $p(t)$ is given by*

$$p(t) = P\{x \in A(t)\} = \int_0^t \theta(u)\mu_n\left(A'(u)\right) du \exp(-\int_0^u \theta(v)\mu_n\left(A'(v) \oplus \check{A}'(u)\right))dv \tag{1c}$$

Proof. The event "$x \in A(t)$" can be written: at some $u < t$, x is covered by a random grain $A'(u)$ falling outside of the previous occurences of grains $A'(v)$ from time 0 to time u (generating a sequential Boolean model with grain $A'(v)$ and with intensity $\theta(v)$). ■

In what follows, we use a family of grains $A'(t)$ with the same shape A' and with size $\lambda(t)$. When A' is a symmetric convex set,

$$\mu_n\left(A'(v) \oplus \check{A}'(u)\right) = \left(\lambda(v) + \lambda(u)\right)^n \mu_n(A'),$$

and $p(t)$ in equation 1c becomes:

$$p(t) = P\{x \in A(t)\} = \int_0^t \theta(u)\lambda^n(u)\mu_n\left(A'\right) du \exp(-\int_0^u \theta(v)\mu_n(A')\left(\lambda(v)+\lambda(u)\right)^n dv) \tag{1d}$$

The aim of the present study is to find some combinations of functions $\theta(v)$ and $\lambda(v)$ providing large values of $p(t)$ derived from equation 1d, with possibly $p(t) \to 1$ for $t \to \infty$. For instance in the case of spherical grains, it is possible by this way to generate a space covering sequence of spheres (that might be composite spheres), as used for instance in physics and mechanics for the so-called Hashin composite spheres model [5].

To generate a random set $A(t)$ with compact grains and to maximize $p(t)$, we decide to use an initial compact grain A' with measure $\mu_n\left(A'\right) = 1$ and a decreasing sequence $\lambda(v)$, with $\lambda(0) = 1$.

3.2. Size distribution of the intact grains. It is possible to compute the "number" $f(\lambda)$ and the "measure" $g(\lambda)$ size distributions of the intact grains. For the "number" size distribution, every grain is counted with the same weight (1), whatever its size. For the "measure" size distribution, every grain is counted proportionally to its measure μ_n.

Using a decreasing sequence $\lambda(u)$, the size is univoquely parametrized by u. We give now the expressions of $f(\lambda(u))$ and of $g(\lambda(u))$.

Theorem 2. *Provided the expression in the denominator below, giving the total number of grains per unit volume, is finite, the "number" size distribution $f(\lambda(u))$ is given by*

$$f(\lambda(u)) = \frac{\theta(u)\exp(-\int_0^u \theta(v)\mu_n(A')\left(\lambda(v)+\lambda(u)\right)^n dv)}{\int_0^\infty \theta(u)du\exp(-\int_0^u \theta(v)\mu_n(A')\left(\lambda(v)+\lambda(u)\right)^n dv)} \tag{1e}$$

Proof. The specific number of intact grains per unit volume appearing between time u and $u+du$ is proportional to $\theta(u)$ and to the probability for the grain with size $\lambda(u)$ to be outside of the Boolean model made of all grains that appeared from time 0 to time u. ■

Theorem 3. *The "measure" size distribution $g(\lambda(u))$ is given by*

$$g(\lambda(u)) = \frac{\theta(u)\lambda^n(u)\mu_n\left(A'\right)\exp(-\int_0^u \theta(v)\mu_n(A')\left(\lambda(v)+\lambda(u)\right)^n dv)}{p(t)} \tag{1f}$$

Proof. The probability $p_i(u)$ to belong to grains with size $\lambda(u)$ is derived from equation 1d:

$$p_i(u) = \theta(u)\lambda^n(u)\mu_n\left(A'\right)\exp(-\int_0^u \theta(v)\mu_n(A')\left(\lambda(v)+\lambda(u)\right)^n dv$$

Normalizing $p_i(u)$ by the overall probability $p(t)$ gives equation 1f ■

4. EXAMPLES OF MODELS OF DENSE PACKING

Some specific cases, obtained for a particular choice of the functions $\theta(u)$ and $\lambda(u)$ used in the model, are detailed now. Of course other choices are possible and would also lead to dense packings. In what follows, numerical calculations and most analytical calculations were made with the software Mathematica.

Packings obtained for an increasing function $\lambda(u)$ show a bounded volume fraction $p(t) < \frac{1}{2^n}$.

To generate a packing with compact grains, decreasing functions $\lambda(u)$ are used, with $\lambda(0) = 1$. To get a dense packing is considered the limit case obtained for $t \to \infty$. The union of all grains appearing between time 0 and time t is a Boolean model $A_1(t)$ with $q_1(t) = 1 - P\{x \in A_1(t)\}$. We have

$$q_1(t) = \exp(-\int_0^t \theta(u)\mu_n(A')\,(\lambda(u))^n\,dv$$

Since by construction $p(t) = P\{x \in A(t)\} < 1 - q_1(t)$, we have to impose $q_1(\infty) = 0$ to get the densest packings with $p(\infty) = p \simeq 1$. Therefore we will make a choice of functions $\theta(u)$ and $\lambda(u)$ satisfying

$$\int_0^\infty \theta(u)\mu_n(A')\,(\lambda(u))^n\,dv = +\infty$$

4.1. Constant rate of implantation. A constant rate of implantation is obtained when $\theta(u)\mu_n(A')\,(\lambda(u))^n = \theta$, as studied in [7]. In that case, $q_1(t) = \exp(-\theta t)$ and $q_1(t) \to 0$ when $t \to \infty$. With this assumptions, equation 1d becomes

$$p(t) = \theta \int_0^t du \exp(-\theta \int_0^u \left(1 + \frac{\lambda(u)}{\lambda(v)}\right)^n dv)$$

and the limit p obtained for $p(t)$ when $t \to \infty$ is given by

$$p = \theta \int_0^\infty du \exp(-\theta \int_0^u \left(1 + \frac{\lambda(u)}{\lambda(v)}\right)^n dv)$$

For the model with a constant rate of implantation, the two size distributions become (dropping the denominator for $f(\lambda(u))$) :

$$f(\lambda(u)) \sim \frac{\theta}{(\lambda(u))^n\,\mu_n(A')} \exp(-\theta \int_0^u \left(1 + \frac{\lambda(u)}{\lambda(v)}\right)^n dv)$$

$$g(\lambda(u)) = \frac{\theta \exp(-\theta \int_0^u \left(1 + \frac{\lambda(u)}{\lambda(v)}\right)^n dv)}{p}$$

For illustration, we consider some case studies in the three-dimensional case.

Case 1: $\lambda(u) = \frac{1}{(1+u)^\alpha}$**.** When $\lambda(u) = \frac{1}{(1+u)^\alpha}$,

$$\int_0^u \left(1 + \frac{\lambda(u)}{\lambda(v)}\right)^3 dv = \int_0^u \left(1 + \left(\frac{1+v}{1+u}\right)^\alpha\right)^3 dv$$

and

$$\begin{aligned}\int_0^u \left(1 + \left(\frac{1+v}{1+u}\right)^\alpha\right)^3 dv \;=\; & \\ & u + \frac{3(u+1)}{\alpha+1} + \frac{3(u+1)}{2\alpha+1} + \frac{u+1}{3\alpha+1} \\ & - \left(\frac{3}{2\alpha+1}\left(\frac{1}{u+1}\right)^{2\alpha} + \frac{1}{3\alpha+1}\left(\frac{1}{u+1}\right)^{3\alpha}\right) \\ & + \frac{3}{\alpha+1}\left(\frac{1}{u+1}\right)^{\alpha}\end{aligned} \tag{2a}$$

From numerical calculations, high concentrations can be obtained for different combinations of θ and α. For instance, $p = 0.909935$ for $\theta = 1$ and $\alpha = 100$; $p = 0.949683$ for $\theta = 0.1$ and $\alpha = 100$; $p = 0.953786$ for $\theta = 0.01$ and $\alpha = 100$. Higher values of θ, in the range $1 - 10$ produce lower volume fractions, decreasing with θ.

To reach very high volume fractions, high coefficients α are required (typically $\alpha = 100$), so that vey small grains have to be generated during the simulation. Typically for $\theta = 0.1$ and $\alpha = 100$, about 150 orders of magnitude of sizes have to be generated with this set of parameters, which is out of reach in practical simulations.

We give in Table 1 the volume fraction reached for $\alpha = 100$ and $\theta = 1$ when stopping the simulations at time t for which $\lambda(t) = 100$, 1000 and 10^6. This last range would correspond to grains in the scales between 1 nm and 1 mm.

$\lambda(t)$	100	1000	10^6
p	0.044	0.066	0.13116

Table 1: Some examples of volume fractions for packings involving a finite range of sizes ($\alpha = 100$ and $\theta = 1$)

Case 2: $\lambda(u) = \exp(-\alpha u)$**.** When $\lambda(u) = \exp(-\alpha u)$, $\int_0^u \left(1 + \frac{\lambda(u)}{\lambda(v)}\right)^3 dv = \int_0^u \left(1 + \exp(-\alpha(u-v))\right)^3 dv$ and

$$\int_0^u \left(1 + \exp(-\alpha(u-v))\right)^3 dv = \frac{29 - 2\exp(-3\alpha u) - 9\exp(-2\alpha u) - 18\exp(-\alpha u) + 6\alpha u}{6\alpha} \tag{2b}$$

Very high values of p are obtained for $\theta = 0.01$ and α in the range $2 - 20$. We get $0.975 < p < 0.996$. For $\alpha = 1$ and $\theta = 0.01$, $p = 0.953185$. For $\alpha = 5$ and $\theta = 0.01$,

$p = 0.990395$. A full covering of space can be theroretically accessed with this model, but a covering fraction of 0.95 requires 131 orders of magnitude for the range of sizes involved in the simulation, which is non realistic in practice.

We give in Table 2 below the volume fraction reached for $\alpha = 1$ and $\theta = 0.01$ when stopping the simulations at time t for which $\lambda(t) = 100$, 1000 and 10^6.

$\lambda(t)$	100	1000	10^6
p	0.0435	0.064	0.1233

Table 2: Some examples of volume fractions for packings involving a finite range of sizes ($\alpha = 1$ and $\theta = 0.01$)

Case 3: $\lambda(u) = \beta + \frac{1}{(1+u)^\alpha}$**.** This variant of Case 1 enables us to generate populations of grains with a finite range of strictly positive sizes, since $\lambda(0) = \beta + 1$ and $\lambda(\infty) = \beta$. When $\beta = 0.1$, the typical range of sizes is around 10, and when $\beta = 0.01$, it is around 100. In the present case, we have

$$\varphi(\beta, u) = \int_0^u \left(1 + \frac{\lambda(u)}{\lambda(v)}\right)^3 dv = \int_0^u \left(1 + \frac{\beta + (1+u)^{-\alpha}}{\beta + (1+v)^{-\alpha}}\right)^3 dv$$

When $\alpha = 1$, we get

$$\begin{aligned}\varphi(\beta, u) \;=\; & \frac{2\beta u(2\beta(u+1)+1)^3 - 6(\beta u + \beta + 1)(2\beta(u+1)+1)}{2\beta^4(u+1)^3} \\ & + \frac{\beta u - 6(\beta u + \beta + 1)(2\beta(u+1)+1)^2 \log(\beta u + \beta + 1) + \beta + 1}{2\beta^4(u+1)^3} \\ & - \frac{(\beta u + \beta + 1)\left(\frac{(\beta u+\beta+1)^2}{(\beta+1)^2} - \frac{6(2\beta(u+1)+1)(\beta u+\beta+1)}{\beta+1} - 6(2\beta(u+1)+1)^2 \log(\beta+1)\right)}{2\beta^4(u+1)^3}\end{aligned}$$

For illustration some calculations were made when $\alpha = 1$. For $\beta = 0.1$, a maximal value $p = 0.198436$ is obtained for $\theta = 0.05$. When $\beta = 0.01$ a maximal value of $p = 0.237714$ is given for $\theta = 0.022$. When $\beta = 0.001$, a maximal value of $p = 0.256222$ is given for $\theta = 0.007$. It seems that no dense packing can be reached with this version of the model.

When $\alpha = 2$, we have

$$\begin{aligned}
\varphi(\beta,u) &= \int_0^u \left(1+\frac{\beta+(1+u)^{-2}}{\beta+(1+v)^{-2}}\right)^3 dv \\
&= \frac{-3\left(25\beta^3(u+1)^6+47\beta^2(u+1)^4+27\beta(u+1)^2+5\right)\tan^{-1}\left(\sqrt{\beta}(u+1)\right)}{8\beta^{7/2}(u+1)^6} \\
&\quad +\frac{8\sqrt{\beta}(u+1)\left(2\beta(u+1)^2+1\right)^3}{8\beta^{7/2}(u+1)^6} \\
&\quad +\frac{-2\sqrt{\beta}(u+1)\left(\beta(u+1)^2+1\right)+3\sqrt{\beta}(u+1)\left(\beta(u+1)^2+1\right)\left(7\beta(u+1)^2+3\right)}{8\beta^{7/2}(u+1)^6} \\
&\quad -\frac{-3\left(25\beta^3(u+1)^6+47\beta^2(u+1)^4+27\beta(u+1)^2+5\right)\tan^{-1}\left(\sqrt{\beta}\right)}{8\beta^{7/2}(u+1)^6} \\
&\quad +\frac{-\frac{2\sqrt{\beta}\left(\beta(u+1)^2+1\right)^3}{(\beta+1)^2}+\frac{3\sqrt{\beta}\left(7\beta(u+1)^2+3\right)\left(\beta(u+1)^2+1\right)^2}{\beta+1}+8\sqrt{\beta}\left(2\beta(u+1)^2+1\right)^3}{8\beta^{7/2}(u+1)^6}
\end{aligned}$$

When $\beta = 0.01$ a maximal value of $p = 0.274566$ is given for $\theta = 0.1$. When $\beta = 0.001$, a maximal value of $p = 0.315167$ is given for $\theta = 0.05$.

No dense packing seems to be obtained with this limitation in the range of sizes.

Case 4: $\lambda(u) = \beta + \exp(-\alpha u)$**.** This variant of Case 2 generates again grains with a finite range of strictly positive sizes. We have

$$\begin{aligned}
\int_0^u \left(1+\frac{\lambda(u)}{\lambda(v)}\right)^3 dv &= \int_0^u \left(1+\frac{\beta+\exp(-\alpha u)}{\beta+\exp(-\alpha v)}\right)^3 dv \\
&= \frac{e^{-3\alpha u}}{2\alpha\beta^3}\left(\beta^3 e^{3\alpha u}(16\alpha u-9)+\beta^2 e^{2\alpha u}(24\alpha u-11)\right. \\
&\quad -\left(\beta e^{\alpha u}+1\right)\frac{\left(2(\beta+1)^2\log(\beta+1)\left(7\beta^2e^{2\alpha u}+5\beta e^{\alpha u}+1\right)-\right)}{(\beta+1)^2} \\
&\quad +\left(\beta e^{\alpha u}+1\right)\frac{\beta\left(9\beta^3e^{2\alpha u}+4\beta^2e^{\alpha u}\left(2e^{\alpha u}+3\right)+\beta\left(10e^{\alpha u}+3\right)+2\right)}{(\beta+1)^2} \\
&\quad +2\left(7\beta^3e^{3\alpha u}+12\beta^2e^{2\alpha u}+6\beta e^{\alpha u}+1\right)\log\left(e^{-\alpha u}+\beta\right) \\
&\quad \left.+2\beta e^{\alpha u}(6\alpha u-1)+2\alpha u\right)
\end{aligned}$$

For $\alpha = 1$ and $\beta = 0.01$, a maximum of $p = 0.313331$ is obtained for $\theta = 0.15$. When $\beta = 0.001$ (involving a range of 1000 in the sizes), a maximum of $p = 0.379635$ is obtained for $\theta = 0.13$. When $\beta = 10^{-4}$, 10^{-5} or 10^{-6}, a maximum of $p = 0.431963$, 0.4735995, 0.459862 is obtained for $\theta = 0.11$, 0.11 , 0.09. Again no highly dense packing is accessed with this range of sizes and this model.

4.2. Examples of time depending rates of implantation. We will consider various cases where $\theta(u)$ and $\lambda(u)$ are respectively an increasing and a decreasing function of u, with the condition $\int_0^\infty \theta(u)\mu_n(A')\left(\lambda(u)\right)^n dv = +\infty$.

Some polynomial laws. When $\theta(u)\mu_n(A') = \theta(1+u)^\beta$ and $\lambda(u) = \frac{1}{(1+u)^\alpha}$, it comes

$$(\lambda(u))^n\theta(u)\mu_n(A') = \theta\frac{(1+u)^\beta}{(1+u)^{n\alpha}}$$

and

$$\begin{aligned}
&\int_0^u (1+v)^\beta \left((1+v)^{-\alpha} + (1+u)^{-\alpha}\right)^3 dv \\
= \;& \frac{2\left(-3\alpha^3 + 20\alpha^2(\beta+1) - 18\alpha(\beta+1)^2 + 4(\beta+1)^3\right)(u+1)^{-3\alpha+\beta+1}}{(\beta+1)(-3\alpha+\beta+1)(-2\alpha+\beta+1)(-\alpha+\beta+1)} \\
& -\frac{(u+1)^{-3\alpha}}{\beta+1} - \frac{3(u+1)^{-2\alpha}}{-\alpha+\beta+1} - \frac{3(u+1)^{-\alpha}}{-2\alpha+\beta+1} - \frac{1}{-3\alpha+\beta+1}
\end{aligned}$$

To get dense packings, we require $\beta \geq n\alpha - 1$. Some typical results for $n = 3$ are given in table 3

θ	0.1	0.01	0.001
$\alpha = 2$, $\beta = 6$	0.317	0.358	0.364
$\alpha = 2$, $\beta = 5.5$	0.414	0.478	

Table 3: Probability p for some sets of parameters

A special case is given for $\beta = n\alpha - 1$ and therefore $\beta = 3\alpha - 1$. We have

$$\begin{aligned}
f(\alpha,u) &= \int_0^u (1+v)^{3\alpha-1}\left((1+v)^{-\alpha} + (1+u)^{-\alpha}\right)^3 dv \qquad (2c)\\
&= \frac{-(u+1)^{-3\alpha} - 6(u+1)^{-2\alpha} + (u+1)^{-\alpha}(6\alpha\log(u+1)+5) + 2}{2\alpha}
\end{aligned}$$

and

$$p = \theta\int_0^\infty \frac{du}{1+u}\exp(-\theta f(\alpha,u))$$

For $\alpha = 1$ and θ increasing from 0.01 to 0.1, p decreases from 0.95 to 0.6. When θ increases from 0.001 to 0.01, p decreases from 0.995 to 0.95.

For $\alpha = 3$, p decreases from 0.999 to 0.985 when θ increases from 0.001 to 0.01.

For $\alpha = 5$, p decreases from 0.9999 to 0.9915 when θ increases from 0.001 to 0.01.

Therefore this special case gives access to extremely high density of packings. As for the previous exponential case, 131 orders of magnitude for the range of sizes are required for a simulation where p reaches 0.95 when $\alpha = 1$ and $\theta = 0.01$, which is practically out of reach.

We give in Table 4 below the volume fraction reached for $\alpha = 1$ and $\theta = 0.01$ when stopping the simulations at time t for which $\lambda(t) = 100$, 1000 and 10^6. They are close to what was obtained for cases 1 and 2 above.

$\lambda(t)$	100	1000	10^6
p	0.04325	0.064	0.1233

Table 4: Some examples of volume fractions for packings involving a finite range of sizes ($\alpha = 1$ and $\theta = 0.01$)

Use of exponential laws for $\lambda(u)$ and $\theta(u)$. When $\lambda(u) = \exp(-\alpha u)$ and $\theta(u)\mu_n(A') = \theta\exp(\beta u)$, we require $\beta \geq n\alpha$ in order to obtain dense packings. In this case, we have

$$p = \theta \int_0^\infty \exp(\beta - 3\alpha) u du \exp\left(-\theta \int_0^u \exp(\beta v)\left(\exp(-\alpha u) + \exp(-\alpha v)\right)^3 dv\right)$$

and (for $\beta \neq 3\alpha$, $\beta \neq 2\alpha$, $\beta \neq \alpha$)

$$\int_0^u \exp(\beta v)\left(\exp(-\alpha u) + \exp(-\alpha v)\right)^3 dv \tag{2d}$$

$$= \frac{\left(6\alpha^3 - 40\alpha^2\beta + 36\alpha\beta^2 - 8\beta^3\right) e^{u(\beta-3\alpha)}}{\beta(\alpha-\beta)(2\alpha-\beta)(3\alpha-\beta)} - \frac{\left(e^{-\alpha u}+1\right)^3 \left(-\frac{3e^{2\alpha u}}{2\alpha-\beta} - \frac{e^{3\alpha u}}{3\alpha-\beta} - \frac{3e^{\alpha u}}{\alpha-\beta} + \frac{1}{\beta}\right)}{\left(e^{\alpha u}+1\right)^3}$$

Typical results for p are given in Table 5, where $\theta = 0.01$. It appears that very dense packings are reached when $\beta \approx n\alpha$.

α	β	p
3	10	0.433
5	16	0.54
5	20	0.266
5	15.1	0.904486
7	21.1	0.929732
7	25	0.34
10	30.01	0.99043

Table 5: Probability p for some sets of parameters in the case of exponential laws

For illustration, the probability $p = 0.93$ is reached for $\alpha = 7$ and $\beta = 21.1$, which requires 99 orders of magnitude in the involved range of sizes, and therefore cannot be implemented in simulations.

Combination of exponential law and of polynomial law. Using $\lambda(u) = \frac{1}{(1+u)^\alpha}$ and $\theta(u) = \theta\exp(\beta u)$, we satisfy $q(\infty) = 0$. We have

$$\varphi(\alpha, \beta, u) = \int_0^u \exp(\beta v)\left((1+v)^{-\alpha} + (1+u)^{-\alpha}\right)^3 dv$$

With this combination, we could not obtain high packing densities.

5. SIZE DISTRIBUTIONS FOR DENSE PACKINGS

It is interesting to derive theoretical size distributions 1f and 1e of grains involved in some cases of previously introduced dense packings.

5.1. Constant rate of implantation and $\lambda(u) = \frac{1}{(1+u)^\alpha}$. The "measure" size distribution is derived from equation 2a, replacing u by its expression in λ. It is given by

$$\begin{aligned} g(\lambda) &= \frac{\theta}{p}\exp(-\theta\left[-1+\lambda^{-\alpha}\left(1+\frac{3}{\alpha+1}+\frac{3}{2\alpha+1}+\frac{1}{3\alpha+1}\right)\right. \\ &\quad \left.-\left(\frac{3\lambda}{\alpha+1}+\frac{3\lambda^2}{2\alpha+1}+\frac{\lambda^3}{3\alpha+1}\right)\right]) \\ \text{for } 0 &\leq \lambda \leq 1 \end{aligned}$$

We have $g(0) = 0$ and $g(1) = \frac{\theta}{p}$. The pdf $g(\lambda)$ increases with λ.
The "number" size distribution is given by

$$\begin{aligned} f(\lambda) &\sim \frac{\theta}{p\mu_n(A')\lambda^3}\exp(-\theta\left[-1+\lambda^{-\alpha}\left(1+\frac{3}{\alpha+1}+\frac{3}{2\alpha+1}+\frac{1}{3\alpha+1}\right)\right. \\ &\quad \left.-\left(\frac{3\lambda}{\alpha+1}+\frac{3\lambda^2}{2\alpha+1}+\frac{\lambda^3}{3\alpha+1}\right)\right] \\ \text{for } 0 &\leq \lambda \leq 1 \end{aligned}$$

We have $f(1) \sim \frac{\theta}{p\mu_n(A')}$, and $f(\lambda) \to \infty$ for $\lambda \to 0$.

5.2. Constant rate of implantation and $\lambda(u) = \exp(-\alpha u)$. The "measure" size distribution is derived from equation 2b, replacing u by its expression in λ.It is given by

$$\begin{aligned} g(\lambda) &= \frac{\theta}{p}\lambda^{\frac{\theta}{\alpha}}\exp\left[-\frac{\theta}{6\alpha}(29-18\lambda-9\lambda^2-2\lambda^3)\right] \\ \text{for } 0 &\leq \lambda \leq 1 \end{aligned}$$

We have $g(1) = \frac{\theta}{p}$ and $g(0) = 0$. The pdf $g(\lambda)$ increases with λ. This is illustrated in Figure 1 for some sets of parameters.

The "number" size distribution is given by

$$\begin{aligned} f(\lambda) &\sim \frac{\theta}{p\mu_n(A')\lambda^3}\lambda^{\frac{\theta}{\alpha}}\exp\left[-\frac{\theta}{6\alpha}(29-18\lambda-9\lambda^2-2\lambda^3)\right] \\ \text{for } 0 &\leq \lambda \leq 1 \end{aligned}$$

We have $f(1) \sim \frac{\theta}{p\mu_n(A')}$. If $\frac{\theta}{\alpha} < 3$, $f(\lambda) \to \infty$ when $\lambda \to 0$. If $\frac{\theta}{\alpha} > 3$, $f(\lambda) \to 0$ when $\lambda \to 0$. If $\theta = 3\alpha$, $f(0) \sim \frac{\theta}{p\mu_n(A')}\exp(-\frac{29}{2})$.

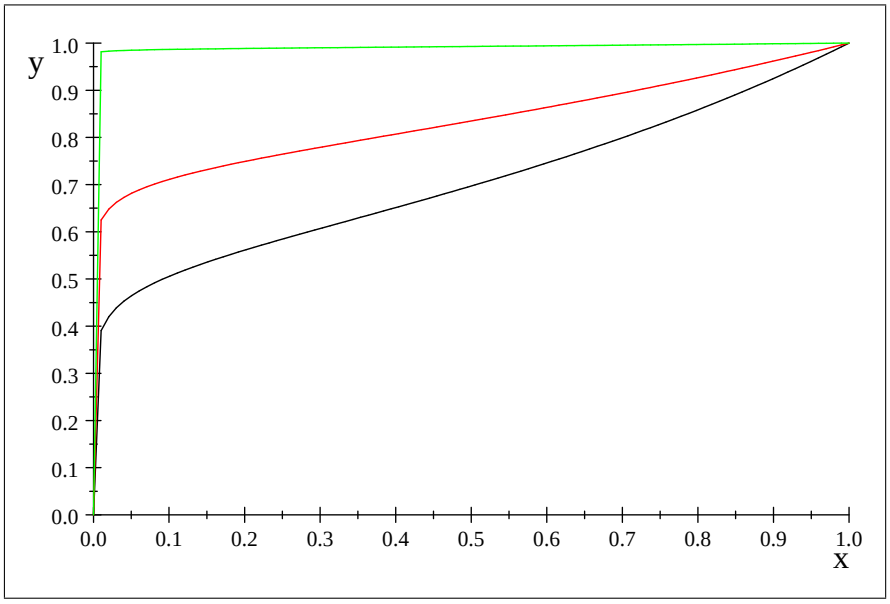

Figure 1: $\frac{p}{\theta}g(\lambda)$ *for* $\theta = 0.1$ *and* $\alpha = 1$ *(black),* $\theta = 0.1$ *and* $\alpha = 2$ *(red),* $\theta = 0.01$ *and* $\alpha = 5$ *(green).*

5.3. Time depending rate of implantation and polynomial law. We consider now the case when $\theta(u)\mu_n(A') = \theta(1+u)^\beta$ and $\lambda(u) = \frac{1}{(1+u)^\alpha}$, with $\beta = 3\alpha - 1$. We get the "measure" size distribution, using equations 1f and 2c

$$\begin{aligned} g(\lambda) &= \frac{\theta}{p}\lambda^{\frac{3\theta\lambda+1}{\alpha}} \exp\left[-\frac{\theta}{2\alpha}(2+5\lambda-6\lambda^2-\lambda^3)\right] \\ \text{for } 0 &\leq \lambda \leq 1 \end{aligned}$$

with $g(1) = \frac{\theta}{p}$ and $g(0) = 0$. The pdf $g(\lambda)$ increases with λ. It is illustrated in Figure 2 for various sets of parameters. They are very different from what was obtained in Figure 1.

The "number" size distribution is given by

$$\begin{aligned} f(\lambda) &\sim \frac{\theta}{p\mu_n(A')\lambda^3}\lambda^{\frac{3\theta\lambda+1}{\alpha}} \exp\left[-\frac{\theta}{2\alpha}(2+5\lambda-6\lambda^2-\lambda^3)\right] \\ \text{for } 0 &\leq \lambda \leq 1 \end{aligned}$$

We have $f(1) \sim \frac{\theta}{p\mu_n(A')}$. If $\alpha > 1/3$, $f(\lambda) \to \infty$ when $\lambda \to 0$. If $\alpha < 1/3$, $f(\lambda) \to 0$ when $\lambda \to 0$. If $\alpha = 1/3$, $f(0) \sim \frac{\theta}{p\mu_n(A')}\exp(-3\theta)$.

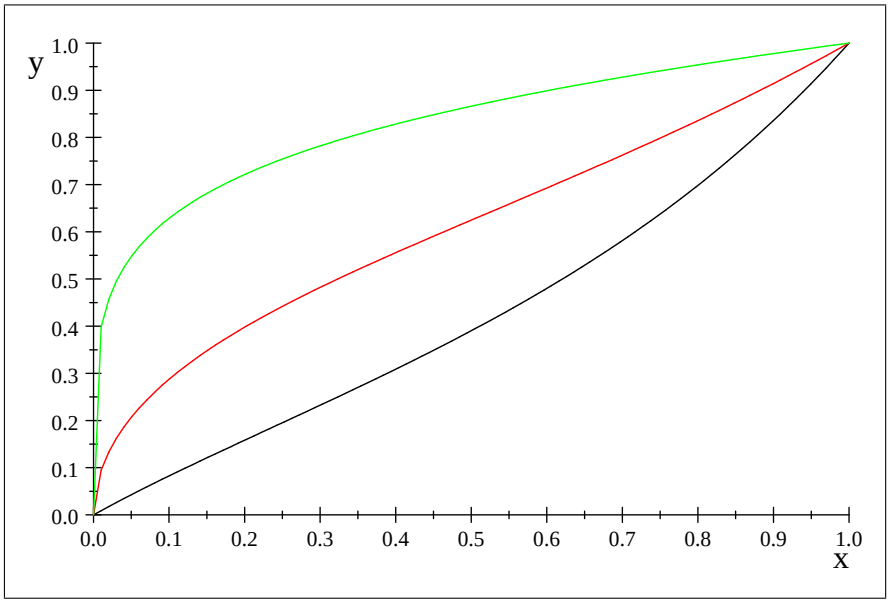

Figure 2: $\frac{p}{\theta}g(\lambda)$ *for* $\theta = 0.1$ *and* $\alpha = 1$ *(black),* $\theta = 0.1$ *and* $\alpha = 2$ *(red),* $\theta = 0.01$ *and* $\alpha = 5$ *(green).*

5.4. Time depending rate of implantation and exponential law. When $\lambda(u) = \exp(-\alpha u)$ and $\theta(u)\mu_n(A') = \theta\exp(\beta u)$, the "measure" size distribution is obtained from equations 1f and 2d:

$$\begin{aligned} g(\lambda) &= \frac{\theta}{p}\lambda^{3-\beta/\alpha}\exp\left\{-\theta\left[\lambda^{3-\beta/\alpha}\frac{\left(6\alpha^3-40\alpha^2\beta+36\alpha\beta^2-8\beta^3\right)}{\beta(\alpha-\beta)(2\alpha-\beta)(3\alpha-\beta)}\right.\right. \\ &\quad \left.\left.-\left(-\frac{1}{3\alpha-\beta}-\frac{3\lambda}{2\alpha-\beta}-\frac{3\lambda^2}{\alpha-\beta}+\frac{\lambda^3}{\beta}\right)\right]\right\} \\ \text{for } 0 &\leq \lambda \leq 1 \end{aligned}$$

with with $g(1) = \frac{\theta}{p}$ and $g(0) = 0$.
The "number" size distribution is given by

$$\begin{aligned} f(\lambda) &\sim \frac{\theta}{p\mu_n(A')}\lambda^{-\beta/\alpha}\exp\left\{-\theta\left[\lambda^{3-\beta/\alpha}\frac{\left(6\alpha^3-40\alpha^2\beta+36\alpha\beta^2-8\beta^3\right)}{\beta(\alpha-\beta)(2\alpha-\beta)(3\alpha-\beta)}\right.\right. \\ &\quad \left.\left.-\left(-\frac{1}{3\alpha-\beta}-\frac{3\lambda}{2\alpha-\beta}-\frac{3\lambda^2}{\alpha-\beta}+\frac{\lambda^3}{\beta}\right)\right]\right\} \\ \text{for } 0 &\leq \lambda \leq 1 \end{aligned}$$

We have $f(1) \sim \frac{\theta}{p\mu_n(A')}$ and $f(\lambda) \to \infty$ when $\lambda \to 0$.

6. PAIR CORRELATION FUNCTION OF INTACT GRAINS CENTERS

For a point process we can define the pair correlation function $G(r)$ as a function of the density ρ (average number of points per unit volume) from [12]:

$$\begin{aligned}\rho^2 G(r)dV_1dV_2 &= P\{\text{ two points of the process are located in the volume elements} \\ &\quad dV_1 \text{ and } dV_2 \text{ centered in two points at the distance } r\}\end{aligned}$$

For a stationary point process, when $r \to \infty$ we get $G(r) \to 1$.

We can derive the pair correlation function $G(r,t)$ of the centres of non-overlapping convex grains A' generated from the dead leaves model (in [13], it is deduced for disks in 2D in the limit area fraction 0.25, using results of Matèrn [10]).

Theorem 4. *In the time non homogeneous case, we have, using a normalization factor k, D being the diameter of $A'(0)$ in the direction of vector h, we get*

$$\begin{aligned}G(h,t) &= 0 \quad \text{for } h < D \\ &\quad kG(h,t) \\ &= 2\int_0^t \theta(u) \int_0^u \theta(w) \exp\left(-\int_0^u \theta(v)\mu_n(A'(u) \cup A'(w)_h) \oplus \check{A}'(v)\right) dv \\ \text{for } h &\geq D\end{aligned}$$

Since for $|h| \to \infty$ we have $G(h,t) \to 1$, we obtain for $h \geq D$

$$G(h,t) = \frac{\int_0^t \theta(u) \int_0^u \theta(w) \exp\left(-\int_0^u \theta(v)\mu_n(A'(u) \cup A'(w)_h) \oplus \check{A}'(v)\right) dv}{\int_0^t \theta(u) \int_0^u \theta(w) \exp\left(-\int_0^u \theta(v)(\mu_n(A'(u) \oplus \check{A}'(v)) + \mu_n(A'(w) \oplus \check{A}'(v))\right) dv} \tag{3a}$$

Proof. Consider the last event concerning point x or point $x+h$: at some time $u < t$, a Poisson point appeared in dV_1 centered in x (or in dV_2 centered in $x+h$), while at some time $\omega < u$ a Poisson point appeared in dV_2 centered in $x+h$ (or in dV_1 centered in x), $A'(u) \cup A'(w)_h$ being outside of the Boolean model generated by grains $A'(v)$ appearing from 0 to u. ■

Corollary 5. *In the case of the time homogeneous model, we get , using a normalization factor k, D being the diameter of A' in the direction of vector h, and with $A'_2 = A' \oplus \check{A}'$*

$$\begin{aligned}G(h,t) &= 0 \quad \text{for } h < D \\ kG(h,t) &= \frac{2}{(\mu_n(A'_2 \cup A'_{2h}))^2}\left[1 - \exp\left(-\theta t \mu_n(A'_2 \cup A'_{2h})\right)\left(1 + \theta t \mu_n(A'_2 \cup A'_{2h})\right)\right] \\ \text{for } h &\geq D\end{aligned}$$

Since for $|h| \to \infty$ we have $G(h,t) \to 1$, we obtain for $h \geq D$

$$G(h,t) = \frac{(2^{n+1}\mu_n(A'))^2}{(\mu_n(A'_2 \cup A'_{2h}))^2} \frac{1 - \exp\left(-\theta t \mu_n(A'_2 \cup A'_{2h})\right)\left(1 + \theta t \mu_n(A'_2 \cup A'_{2h})\right)}{1 - \exp\left(-\theta t 2^{n+1}\mu_n(A')\right)\left(1 + \theta t 2^{n+1}\mu_n(A')\right)} \tag{3b}$$

Equation 3b can be written in a more condensed way. We put $q = \exp(-\theta t 2^n \mu_n(A'))$ and therefore we have $p(t) = \frac{1}{2^n}(1-q)$ (q is the probability to be outside of the Boolean model with grains A'_2, generated from 0 to t). We use

$$\begin{aligned} K_2(h) &= \mu_n(A'_2 \cap A'_{2h}) \\ r_2(h) &= K_2(h)/K_2(0) \end{aligned}$$

We get

$$\begin{aligned} G(h) &= 0 \text{ for } h < D \\ G(h) &= \left(\frac{2}{2-r_2(h)}\right)^2 \frac{1-q^{2-r_2(h)}(1-\log(q)(2-r_2(h)))}{1-q^2(1-\log(q)} \text{ for } h \geq D \end{aligned} \tag{3c}$$

The limiting case is obtained for $p = 1/2^n$ (or equivalently $q = 0$ and $t \to \infty$):

$$\begin{aligned} G(h) &= 0 \text{ for } h < D \\ G(h) &= \left(\frac{2}{2-r_2(h)}\right)^2 \text{ for } h \geq D \end{aligned} \tag{3d}$$

In $\mathbb{R}$, if A' is the segment with length 1, we have $r_2(h) = 1 - \frac{h}{2}$ for $h \leq 2$. It comes

$$\begin{aligned} G(h) &= 0 \text{ for } h < 1 \\ G(h) &= \left(\frac{2}{1+h/2}\right)^2 \frac{1-q^{1+h/2}(1-\log(q)(1+h/2))}{1-q^2(1-\log(q)} \text{ for } 1 < h < 2 \\ G(h) &= 1 \text{ for } h \geq 2 \end{aligned} \tag{3e}$$

We get

$$G(1) = \frac{16}{9}\frac{1-q^{3/2}(1-\frac{3}{2}\log(q))}{1-q^2(1-\log(q)}$$

so that there is a strong influence of the volume fraction on the shape of $G(r)$.

For non overlapping disks with radius R in the two-dimensional space, we have to use equation 3c with $D = 2R$ and

$$\begin{aligned} r_2(h) &= \frac{K(h)}{K(0)} = \arccos(\frac{h}{4R}) - \frac{h}{4R}\sqrt{1-(\frac{h}{4R})^2} \text{ for } h \leq 4R \\ r_2(h) &= 0 \text{ for } h \geq 4R \end{aligned}$$

For spherical grains with radius R in the three-dimensionnal space, we have

$$\begin{aligned} r_2(h) &= 1 - \frac{3h}{8R} + \frac{h^3}{128R^3} \text{ for } h < 4R \\ r_2(h) &= 0 \text{ for } h \geq 4R \end{aligned}$$

7. Conclusion

Intact grains of the dead leaves model provide packings with a volume fraction controlled by a wise combination of the time sequence of density $\theta(t)$ and of sizes $\lambda(t)$. Using similar convex grains symmetrical with respect to the origin, very dense packings can be theoretically obtained, up to a full covering of space by non-overlapping convex grains, a particular case being spherical grains. Considering convex cells delimited by the boundaries of grains, tessellations of space with compact convex cells are generated for appropriate sequences asymptotically leading to a full covering of space. Models with different grain size distributions are obtained by this process. Packings with extremal volume fractions (close to 1) involve huge ranges of sizes (the smallest diameters of grains tending to 0), which is theoretically feasible, but practically out of reach of computer simulations.

References

[1] Altendorf H., Jeulin D. (2011) Random-walk-based stochastic modeling of three-dimensional fiber systems, Physical Review E 83, 041804.

[2] Andersson J., Häggström O., Månsson M. (2006) The volume fraction of a non-overlapping germ-grain model, - Electronic Communications in Probability, 11, pp. 78-88.

[3] Aste T., Weaire D. 2000) The pursuit of perfect packing, Institute of Physics Publisher.

[4] Delarue A., Jeulin D. (2001) Multi-scale simulations of spherical aggregates, communication to the 8th European Congress for Stereology, Bordeaux, 4-7 September 2001, Image Analysis and Stereology, Vol. 20, N 3, pp. 181-186.

[5] Hashin Z. (1962) The elastic moduli of hetrogeneous materials, Journal of Applied Mechanics, Vol. 29, N°1, pp. 143–150.

[6] Jeulin D. (1980) Multi-component random models for the description of complex microstructures, Proc. 5th International Congress for Stereology, Mikroskopie, Vol. 37 S: 130-137.

[7] Jeulin D. (1998) Random packings, unpublished work.

[8] Jeulin D. (1998) Probabilistic models of structures, Invited Key-Note Lecture, Workshop PROBAMAT 21rst Century, Perm, Russia, 10-12 September 1997 , G.N. Frantziskonis (ed), NATO ASI Series vol. 46, 233-257.

[9] Kiderlen M., Hörig M. (2013) Matérn's hard core models of types I and II with arbitrary compact grains, CSGB Research report N°5, July 2013.

[10] Matérn B. (1960) Spatial Variation, Meddelanden fran Statens Skogsforkningsinstitut, Vol. 49 (5), pp. 1-144.

[11] Matheron G. (1968) Schéma booléen séquentiel de partition aléatoire, Paris School of Mines Publication.

[12] Stoyan, D., Kendall, W.S., Mecke, J. Stochastic Geometry and its Applications, J. Wiley, New York, 1987.

[13] Stoyan D., Schlather M. (2000) Random Sequential Adsorption: relationship to Dead Leaves and Characterization of Variability, Journal of Statistical Physics, Vol. 100, N° 5/6, pp. 969-979.